

Damian Miara, Jolanta Matusiak

Effect of Welding Conditions on the Structure and Properties of Joints Made of Wrought Aluminium Alloys in High-Speed FSW

Abstract: The FSW process is primarily used to join elements made of similar materials. Generally, the making of structures involving the use of similar materials require low welding rates. The article presents research results connected with the high-speed FSW of wrought aluminium alloys and the effect of welding conditions on the structure and properties of joints. The welds made within the research-related tests were characterized by high quality and free from any imperfections.

Keywords: Friction Stir Welding, wrought aluminium alloys

DOI: [10.17729/ebis.2018.5/12](https://doi.org/10.17729/ebis.2018.5/12)

Introduction

The making of lightweight and, at the same time heavy-duty, structures continues to pose a significant challenge for various industries including the automotive, aviation or the ship-building sector. The development of the above-named structures entails the search for innovative methods making it possible to join similar and dissimilar structural materials. A relatively important factor when making the aforesaid joints is joining efficiency. One of the methods which can be used in the making of such joints and which can be referred to as innovative, primarily because of the wide range of joinable materials, is friction welding with the stirring of the weld materials, also known as Friction Stir Welding (FSW) [1].

Previous research results concerning the FSW method have revealed that the formation of the FSW weld and the mechanical properties

of the FSW joint are primarily affected by the type of a welding tool, its shape and dimensions [2]. In addition, the quality of welds is influenced by process parameters, including the tool rotation rate and the welding rate. The tool rotation rate affects the stirring of materials around the probe. The higher the rate, the more mixed the material in the central area of the weld and the smaller the grain size are. [3]. The welding rate affects the process efficiency and is adjusted in relation to types of materials and structural joint-related requirements. The FSW process performed using welding rates exceeding 800 mm/min can be categorised as high-speed FSW. Taking into consideration the prospective potential of the FSW technology in production conditions, it is becoming important to develop the welding technology not only in relation to the obtainment of joints characterised by appropriate functional properties

mgr inż. Damian Miara (MSc Eng.); dr inż. Jolanta Matusiak (PhD (DSc) Eng.) – Instytut Spawalnictwa, Department of Resistance and Friction Welding and Environmental Engineering

Table 1. Chemical composition of aluminium alloy EN AW-6082 used in the tests [4]

No.	Designation	Contents of chemical elements, %								
		Si	Cu	Mg	Mn	Fe	Ti	Cr	Zn	Al
1	EN AW-6082 (PA4)	0.7-1.3	≤0.1	0.6-1.2	0.4-1.0	≤0.5	≤0.1	≤0.2	≤0.2	rest

but also in terms of appropriately fast making of the joints.

Table 2. Selected mechanical properties of aluminium alloy EN AW-6082 [4]

No.	Designation	Minimum properties		
		$R_{p0,2}$ MPa	R_m MPa	A_{50} , %
1.	EN AW-6082 (PA4)	255	300	9

Test materials, test rig and testing methodology

The FSW technological tests of butt joints involved the use of 6 mm thick plates made of wrought aluminium alloy EN AW-6082. The above-named alloy is characterised by high mechanical strength and toughness, medium fatigue strength and machinability, good corrosion resistance and polishability. The alloy is commonly used in the machine-building industry, where mechanical requirements are stricter than those concerning the 5000 series

alloys. Wrought aluminium alloy EN AW-6082 is used in load-bearing elements of lorries, buses, trailers, ships, cranes, railway cars, bridges and guard rails.

The tests involved the use of two taper-threaded tools, one of which was a Triflute™ type of tool (Table 3). The tests concerning the FSW of aluminium alloy EN

Table 3. Shape and dimensions of the tools used in the test

Tool	Schematic drawing
Triflute type tapered tool with the flat tip of the probe	
Tapered tool with the flat tip of the probe	



Fig. 1. Welding station (FSW) used in the tests: a) conventional milling machine: FYF32JU2, b) welding machine fixtures: clamps fixing the workpieces

AW-6082 were performed within a wide range of welding process parameters. The tool rotation rates $V_n = 450, 710, 900, 1120, 1400$ and 1800 rpm were combined with two welding rates $V_z = 900$ and 1120 mm/min. During the welding process, the friction surface of the shoulder was positioned at an angle of 1.5° in relation to plates subjected to welding.

The welding process was performed using an FSW machine based on a FYF32JU2 conventional milling machine (JAFO S.A.) (see Fig. 1) provided with clamps fixing workpieces.

Measurements of joint rupture force F_m [kN] were performed using an INSTRON 4210 testing machine and based on the PN-EN ISO 4136:2013-05 standard [5]. To determine the effect of the FSW process parameters on the stirring of the material, the cross-sections of the joints were subjected to macroscopic

metallographic tests performed in accordance with the 17639:2013-12 standard [6].

Test results

Visual tests

The tests related to the possibility of making welds at a welding rate higher than 800 mm/min revealed that it was possible to make such joints within the entire tested (extensive) range of welding process parameters. Both on the face and root side, the welds were characterised by the shape typical of the FSW method. On the face side it was possible to notice characteristic semicircles. The welds were regular in shape, with a small amount of material outside the weld (in most of the cases – on the retreating side). Figures 2-7 present examples welds on the face side.



Fig. 2. FSW butt weld made of aluminium alloy EN AW-6082; welding parameters: $V_n = 450$ rpm, $V_z = 1120$ mm/min; Triflute type tapered tool [7, 8]



Fig. 3. FSW butt weld made of aluminium alloy EN AW-6082; welding parameters: $V_n = 1120$ rpm, $V_z = 1120$ mm/min; Triflute type tapered tool [7, 8]



Fig. 4. FSW butt weld made of aluminium alloy EN AW-6082; welding parameters: $V_n = 1800$ rpm, $V_z = 1120$ mm/min; Triflute type tapered tool [7, 8]



Fig. 5. FSW butt weld made of aluminium alloy EN AW-6082; welding parameters: $V_n = 450$ rpm, $V_z = 1120$ mm/min; tapered tool [7, 8]



Fig. 6. FSW butt weld made of aluminium alloy EN AW-6082; welding parameters: $V_n = 1120$ rpm, $V_z = 1120$ mm/min; tapered tool [7, 8]



Fig. 7. FSW butt weld made of aluminium alloy EN AW-6082; welding parameters: $V_n = 1800$ rpm, $V_z = 1120$ mm/min; tapered tool [7, 8]

In relation to a rotation rate and welding rate, the outside appearance of the welds differed slightly; the welds were characterised by regular shapes. An increase in a tool rotation rate resulted in an increase in the stirring of the material as well as in an increase in the amount and size of material flashes (primarily on the retreating side). The sizes of the flashes also depended on the depth of the tool penetration in the materials being joined.

Measurements of forces and torque

During the welding process the Lowstir head was used to record the following process parameters:

- pressure force – force with which the tool affected the material along the normal to the surface of the plates subjected to welding; the aforesaid force is necessary for maintaining the position of the shoulder above the surface of the materials subjected to welding,
- force in the direction of welding – force acting in parallel to the movement of the tool,
- torque – required for the tool to rotate during the welding

process; the value of torque depends on the pressure force and friction coefficient.

Table 4 and 5 present the mean values of forces and torque recorded during welding in the stabilised state. An exemplary graph presenting the forces and the torque during the welding process is depicted in Figure 8.

The comparison of values of force in the direction of welding, welding pressure force and torque in relation to various values of the tool rotation rate revealed that, in general, an increase in the tool rotation rate was accompanied by a decrease in welding pressure force and that in torque. However, it was possible to notice a deviation from the regular course of force in the direction of welding (which should

Table 4. Values of forces and torque recorded during the welding process of plates made of aluminium alloy EN AW-6082, performed using the Triflute type tapered tool and welding rate $V_z=1120$ mm/min [8]

No.	Welding parameters		Force in the direction of welding, kN	Welding pressure force, kN	Torque, Nm
	V_n , rpm	V_z , mm/min			
1.	450	1120	3.17	38.54	148.24
2.	710	1120	1.40	32.84	107.69
3.	900	1120	1.61	34.45	84.03
4.	1120	1120	1.99	31.45	62.04
5.	1400	1120	1.78	27.13	49.72
6.	1800	1120	2.78	29.45	43.45

be consistent with the tendency of changes in pressure force and torque). At the lowest tool rotation $V_n = 450$ rpm, the values of the above-named forces were very high. An increase in the tool rotation rate to $V_n = 710$ rpm was accompanied by a decrease in the force in the direction of welding (in some cases by more than a half - Table 4 - items 1 and 2). A further increase in the tool rotation rate was accompanied by an increase in force in the direction of welding. The above-named dependences referred to each tool and various welding rates. In general, the values of forces in the direction of welding, pressure forces and torque depended, among other things, on the depth to which the material was penetrated by the welding tool. When using a manually controlled welding machine during welding, it is very difficult to precisely identify correlations between individual values of forces and torque.

Tensile tests

The quality of the FSW joints obtained using various welding parameters was assessed on the basis of static tensile test results. The detailed analysis of the tensile strength test results involved statistical inference based on the standard deviation (σ), identifying by how much all of the tensile strength values differed (on average) from the arithmetic mean of the variable being tested. The values of tensile strength tests (for 5 specimens in a lot) in relation to various tools and various welding rates are presented in Tables 6 and 7.

Table 5. Values of forces and torque recorded during the welding process of plates made of aluminium alloy EN AW-6082 performed using the tapered tool and welding rate $V_z=1120$ mm/min [8]

No.	Welding parameters		Force in the direction of welding, kN	Welding pressure force, kN	Torque, Nm
	V_n , rpm	V_z , mm/min			
1.	450	1120	4.58	38.91	132.50
2.	710	1120	2.17	35.41	101.61
3.	900	1120	1.95	33.76	80.03
4.	1120	1120	1.86	34.32	66.00
5.	1400	1120	2.08	30.05	50.82
6.	1800	1120	2.95	31.61	43.27

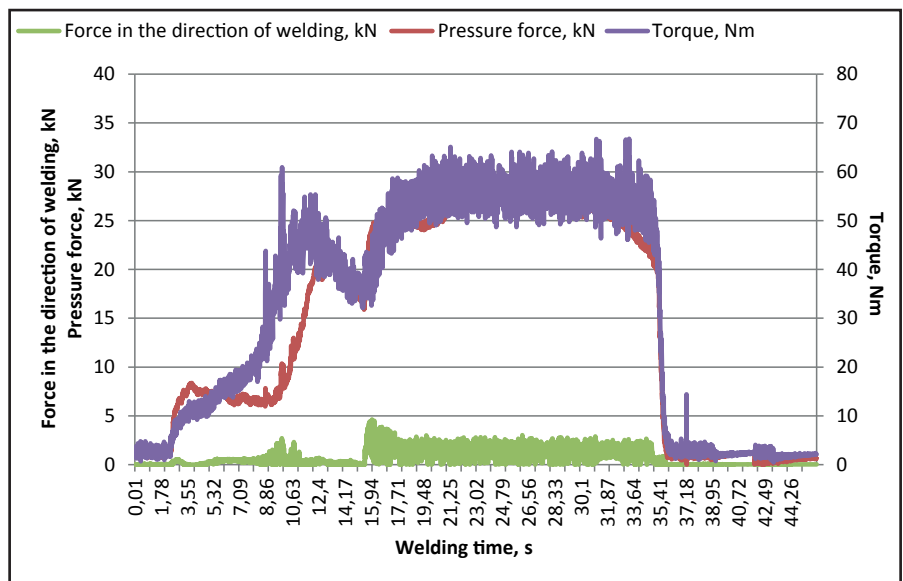


Fig. 8. Force in the direction of welding, pressure force and torque recorded during the welding of plates made of aluminium alloy EN AW-6082; welding parameters: $V_n = 1120$ rpm, $V_z = 1120$ mm/min; Triflute type tapered tool [8]



Fig. 9. Exemplary specimen after the tensile test; welding parameters: $V_n = 1800$ rpm and $V_z = 1120$ mm/min [8]

An exemplary FSW specimen after the tensile test is presented in Figure 9.

The mean tensile strength changed in relation to the tool rotation rate (the tendency of changes was similar in cases of welding rate changes). The lowest tool rotation rate, i.e. $V_n = 450$ rpm, was related to the lowest values of mean tensile strength of the welds – regardless of the welding rate and the tool. Also in

Table 6. Tensile test results in relation to the welds made of aluminium alloy EN AW-6082; Triflute type tool; welding rate $V_z = 1120$ mm/min [7, 8]

No.	Tool rotation rate V_n , rpm	Tensile strength R_m , MPa	Area of rupture	Mean tensile strength $R_{aver.}$, MPa	Standard deviation, σ	Variation coefficient
1.	450	205	Rupture in the weld axis	203	2,29	0,01
2.		200	Rupture in the weld axis			
3.		203	Rupture in the weld axis			
4.		202	Rupture in the weld axis			
5.	710	245	Rupture in the weld axis	246	2,13	0,01
6.		249	Rupture in the weld axis			
7.		247	Rupture in the weld axis			
8.		244	Rupture in the weld axis			
9.	900	241	Rupture in the weld axis	245	3,86	0,02
10.		245	Rupture in the weld axis			
11.		250	Rupture in the weld axis			
12.		243	Rupture in the weld axis			
13.	1120	249	Rupture on the advancing side	252	3,90	0,02
14.		255	Rupture on the advancing side			
15.		248	Rupture on the advancing side			
16.		256	Rupture on the advancing side			
17.	1400	261	Rupture on the retreating side	258	3,19	0,01
18.		260	Rupture on the advancing side			
19.		254	Rupture in the weld axis			
20.		258	Rupture on the retreating side			
21.	1800	247	Rupture in the weld axis	251	10,70	0,04
22.		260	Rupture on the advancing side			
23.		238	Rupture in the weld axis			
24.		259	Rupture on the advancing side			

relation to the tool rotation rate amounting to 710 rpm in some cases it was possible to notice significantly lower values of mean tensile strength of the welds. In most cases, also the highest tool rotation rate was accompanied by a decrease in the mean tensile strength of the welds. However, the aforesaid decrease was not as significant as in relation to the lowest tool rotation rate, i.e. 450 rpm. The tensile test results combined with results concerning forces and torque disqualified the lowest (450 rpm) and the highest (1800 rpm) tool rotation rate as precluding the obtainment of welds characterised by appropriate and repeatable quality. The tool rotation rate amounting to 710 rpm was also recognised as unfavourable because

of not sufficiently plasticised materials being joined.

Macroscopic metallographic tests

Selected specimens were subjected to macroscopic metallographic tests related to the weld structure. The preparation of specimens for the macro and microscopic metallographic tests involved cutting the welds out of the joints in a manner enabling the obtainment of the cross-section of the test welds. Figures 10-12 present the macrostructures of selected welds in relation to the tool rotation rate.

The exemplary macrostructures of the welds presented in the figures revealed the joint area characterised by the full metallic continuity in

Table 7. Tensile test results in relation to the welds made of aluminium alloy EN AW-6082; tapered tool; welding rate $V_z = 1120$ mm/min [7, 8]

No.	Tool rotation rate V_n , rpm	Tensile strength R_m , MPa	Area of rupture	Mean tensile strength $R_{aver.}$, MPa	Standard deviation, σ	Variation coefficient
1.	450	194	Rupture in the weld axis	185	14.14	0.08
2.		185	Rupture in the weld axis			
3.		195	Rupture in the weld axis			
4.		165	Rupture in the weld axis			
5.	710	260	Rupture in the weld axis	261	0.50	0.00
6.		261	Rupture on the retreating side			
7.		260	Rupture on the retreating side			
8.		261	Rupture on the retreating side			
9.	900	263	Rupture on the advancing side	265	2.66	0.01
10.		265	Rupture on the retreating side			
11.		262	Rupture on the advancing side			
12.		268	Rupture on the retreating side			
13.	1120	256	Rupture on the retreating side	259	2.55	0.01
14.		261	Rupture on the advancing side			
15.		261	Rupture on the advancing side			
16.		257	Rupture on the advancing side			
17.	1400	264	Rupture on the advancing side	266	1.57	0.01
18.		267	Rupture on the advancing side			
19.		268	Rupture on the advancing side			
20.		267	Rupture on the advancing side			
21.	1800	265	Rupture on the advancing side	263	1.77	0.01
22.		262	Rupture on the advancing side			
23.		262	Rupture on the advancing side			
24.		264	Rupture on the advancing side			

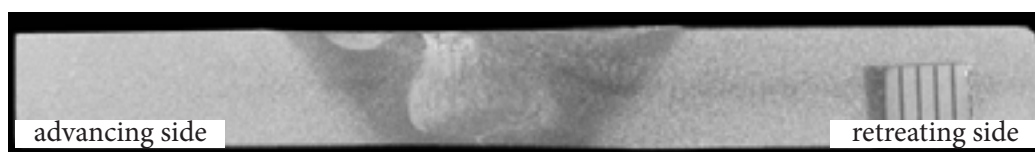


Fig. 10. Macrostructure of the FSW weld made of aluminium alloy EN AW-6082; welding parameters $V_n = 450$ rpm, $V_z = 1120$ mm/min; Triflute type tapered tool; etchant: Keller's reagent [8]

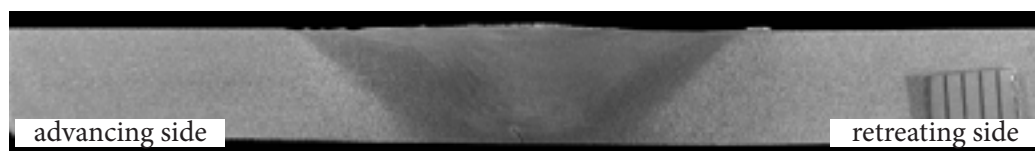


Fig. 11. Macrostructure of the FSW weld made of aluminium alloy EN AW-6082; welding parameters $V_n = 1120$ rpm, $V_z = 1120$ mm/min; Triflute type tapered tool; etchant: Keller's reagent [8]

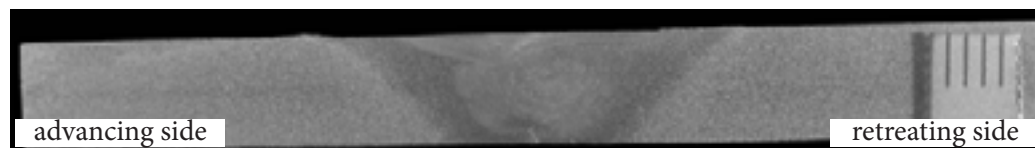


Fig. 12. Macrostructure of the FSW weld made of aluminium alloy EN AW-6082; welding parameters $V_n = 1800$ rpm, $V_z = 1120$ mm/min; Triflute type tapered tool; etchant: Keller's reagent [8]

relation to all of the welding process parameters. In each specimen it was possible to notice the zone deformed thermomechanically by the shoulder, the weld nugget and the heat affected zone (both on the advancing and re-treating side). The shape of the welds was trapezoid, regardless of the applied combination of welding process parameters. In cases of some specimens it was possible to notice the lack of penetration on the root side.

The research-related tests also involved macroscopic metallographic observations of selected welds. The objective of the tests was to identify the degree of the stirring of materials in relation to the welds formed in the stabilised state, in the cross-sections of horizontal planes in relation to the surface of the plates subjected to welding. To this end, a 40 mm long section of the weld was subjected to milling to “remove” subsequent layers of the material millimetre after millimetre (across the entire 6 mm thickness of the plates being welded), starting from the weld face side. The schematic presentation of sampling the successive layers for macroscopic metallographic tests of successive surfaces of the weld is shown in Figure 13. The subsequent figures present the test results in the form of macrostructures of the successive layers of the weld surface. The tests involved the welds made using the Triflute type tapered tool. The tests results in relation to the specimen made using the tool rotation rate $V_n = 1120$ rpm and a welding rate of 1120 mm/min is presented in Figure 14.

The test concerning the macrostructures of successive layers of the weld surface made it possible to determine the manner in which the structure of

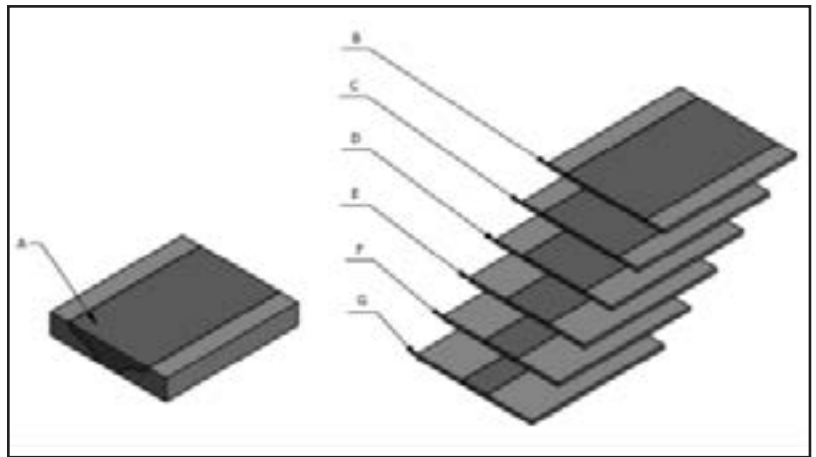


Fig. 13. Schematic preparation of successive layers of the weld surface for macroscopic metallographic tests [8]

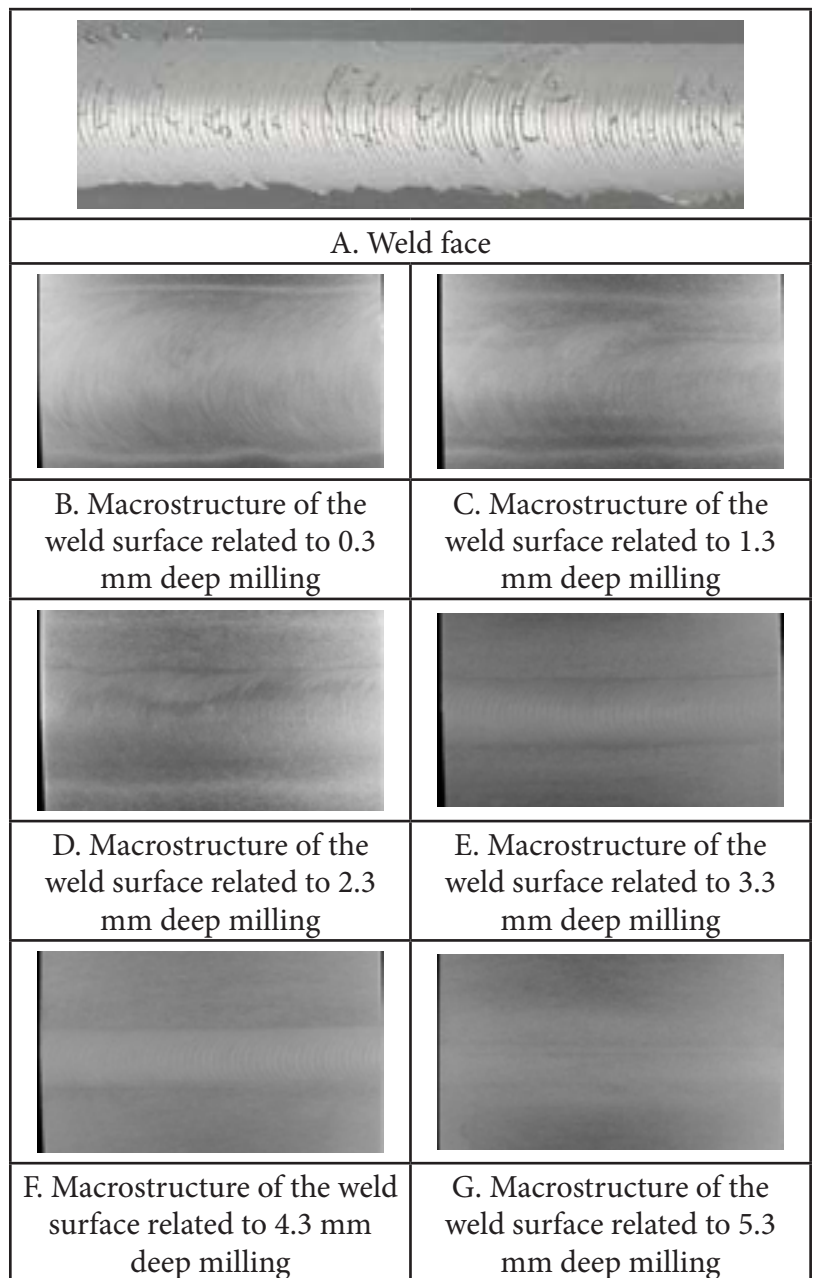


Fig. 14. Macrostructures of individual layers of the weld subjected to milling on the weld face side in accordance with the schematic diagram presented in Figure 10; welding parameters $V_n = 1120$ rpm, $V_z = 1120$ mm/min; Triflute type tapered tool; etchant: Keller’s reagent [8]

the entire weld area was formed across the depth affected by the welding tool in relation to its rate of rotation. It was ascertained that various rates of rotation led to variously formed structures of individual planes of the weld – also in relation to those areas of the weld which were not subjected to the tests because of the milling of successive layers of the weld at a distance of 1 mm (and not shorter). The unequivocal determination of the weld structure (obtained using various rates of rotation) proved difficult in comparison and requires further research.

In addition, to fully present the image of the weld, i.e. not only in the plane form, it was necessary to perform additional macroscopic metallographic tests in order to identify the weld structure in the central welding area being of 40 mm in length and located precisely in the weld axis. The preparation of the joint is presented schematically in Figure 15. The additional tests enabled the viewing of the material structure in the area below 5.3 mm in relation to the weld axis (Fig. 16).

The results of the above-presented tests revealed that the materials were fully stirred and

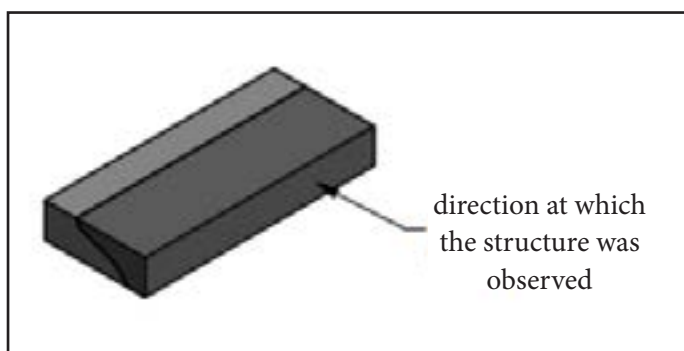


Fig. 15. Schematic diagram of the preparation of the joint for macrostructural tests across the weld along its axis [8]

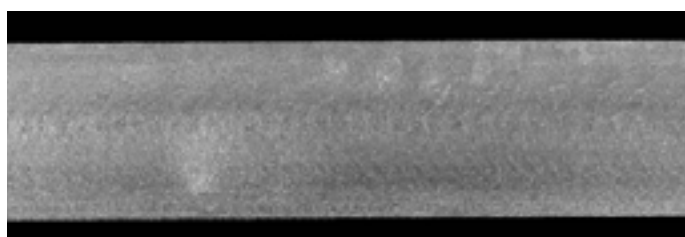


Fig. 16. Macrostructure of the weld along the weld axis, in the stabilised welding state; welding parameters $V_n = 1120$ rpm, $V_z = 1120$ mm/min; Triflute type tapered tool; etchant: Keller's reagent [8]

that the weld was continuous in the entire area. All of the macrostructures clearly revealed differences in the effect of the tool probe. It was also noticed that the structure of the weld was similar regardless of an area subjected to observation (cut plane).

However, regardless of types of tests, including a tool rotation rate or a welding rate, the structure of the weld in the area affected by the probe was similar. In the area of the face and that of the root the structure of the welds varied. This resulted from the various degree of the stirring of the same batch of materials at the same time, which, in turn was directly related to the rate of tool rotation, and, consequently, to the temperature in the welding area.

Concluding remarks

1. The use of tool rotation rate $V_n = 900, 1120$ and 1400 rpm in combination with two welding rates, i.e. $V_z = 900$ and 1120 mm/min enabled the obtainment of high quality welds, i.e. fully plasticised, metallurgically continuous and characterised by high tensile strength.
2. The use of tool rotation rate $V_n = 450$ and 1800 rpm in combination with two welding rates, i.e. $V_n = 900$ and 1120 mm/min did not make it possible for the welds to obtain sufficiently high strength. The above-named tool rotation rate values did not enable the obtainment of proper welds during the high-speed FSW of aluminium alloy EN AW-6082.

References

- [1] Bhadeshia H.K.D.H.: "Friction Stir Welding", Cambridge, 2002.
- [2] Elangovan K., Balasubramanian V., and Babu S.: Developing an Empirical Relationship to Predict Tensile Strength of Friction Stir Welded AA2219 Aluminum Alloy. *Journal of Materials Engineering and Performance*, 2008, no. 820, vol. 17(6).
- [3] Rajiv S., Mishra A, Murray W. Mahoney E.: *Friction stir welding and processing*. ASM International, 2007.

- [4] PN-EN 573-3:2014-02. Aluminium i stopy aluminium - Skład chemiczny i rodzaje wyrobów przerobionych plastycznie - Część 3: Skład chemiczny i rodzaje wyrobów.
- [5] PN-EN ISO 4136:2013-05E. Badania niszczące złączy spawanych metali - Próba rozciągania próbek poprzecznych.
- [6] PN-EN ISO 17639:2013-12. Badania niszczące spawanych złączy metali - Badania makroskopowe i mikroskopowe złączy spawanych.
- [7] Praca badawcza nr ST-362/M. Rozpoznawcze badania wysokowydajnego zgrzewania FSW stopu aluminium przerabianego plastycznie. Instytut Spawalnictwa, 2016.
- [8] Praca badawcza nr ST-366/17/ZR (Bb-125). Badania wpływu warunków zgrzewania na strukturę i własności złączy ze stopu aluminium przerabianego plastycznie przy wysokowydajnym zgrzewaniu metodą FSW. Instytut Spawalnictwa, 2017.